Available online at www.sciencedirect.com
SCIENCE DIRECT
Talanta 69 (2006) 572–580
Talanta
www.elsevier.com/locate/talanta

Microanalysis of oligodeoxynucleotides by cathodic stripping voltammetry at amalgam-alloy surfaces in the presence of copper ions

Stanislav Hasoň *, Vladimír Vetterl

Institute of Biophysics, Academy of Science of the Czech Republic, Královopolská 135, CZ-612 65 Brno, Czech Republic

Received 13 May 2005; received in revised form 4 October 2005; accepted 25 October 2005
Available online 28 November 2005

Abstract

The application of gold amalgam-alloy electrode (AuAE) for a sensitive voltammetric detection of different oligodeoxynucleotides (ODNs) containing the purine units within the ODN-chains in the presence of copper is described. The detection of ODNs is based on the following procedure: (i) the first step includes an acidic hydrolysis of the ODN (ahODN) samples performing the release of the purine bases from ODN-chain; (ii) the second step includes an electrochemical accumulation of the complex of the purine base residues released from ODN-chain with copper ions Cu(I) (ahODN–Cu(I) complex) at the potential of reduction of copper ions Cu(II) on the amalgam-alloy electrode surfaces; (iii) finally followed the cathodic stripping of the electrochemically accumulated ahODN–Cu(I) complex from the electrode surface. The proposed electrochemical method was used for: (a) detection of different ODN lengths containing only adenine units (the number of adenine units within the ODN-chains was changed from 10 to 80), and (b) determination of the number of purine units within the 30-mer ODNs containing a random sequence segments involving both the purine and pyrimidine units. The intensity of the cathodic stripping current density peak (j_{CSP}) of the electrochemically accumulated ahODN–Cu(I) complex increased linearly with the increasing number of purine units within the ODN-chains. We observed a good correlation between the percentage content of purine units to the whole length of different 30-mer ODNs and the percentage content of the intensity of the j_{CSP} of the electrochemically accumulated 30-mer ahODN–Cu(I) complexes. The detection of acid hydrolysed 80-mer (A_{80}) in the bulk solution and in a 20-μl volume is possible down to 200 pM and 2 nM at the AuAE, respectively. For the shortest 10-mer (A_{10}) a detectable value of 5 nM in the bulk solution on the AuAE was observed. The sensitive detection of different ODNs containing the purine units in their chains in the presence of copper can be also performed at the platinum amalgam-alloy (PtAE) and copper amalgam-alloy (CuAE) contrary to a lower sensitivity at the silver amalgam-alloy (AgAE) electrode.
© 2005 Elsevier B.V. All rights reserved.

Keywords: Gold amalgam-alloy electrode; Platinum amalgam-alloy electrode; Silver amalgam-alloy electrode; Copper amalgam-alloy electrode; Oligodeoxynucleotides; Purine base residue–copper(I) complex; Analysis of microliter volumes of oligodeoxynucleotides

1. Introduction

Application of electrochemical techniques in nucleic acids analysis and in development of DNA biosensors is one of the major topics of the present nucleic acid electrochemistry due to the fact that the electrochemical signal transduction appears to be a useful alternative to the optical one mainly due to lower costs, simple design, small dimension and easily operability of these devices [1–3]. Electrochemical analysis of nucleic acids has employed various electrode materials that proved to be suitable in different types of measurements [4–6]. At mercury and carbon electrodes unmodified DNA produce reduction and/or oxidation signals due to purine and pyrimidine base residues. All nucleic acid bases form sparingly soluble compounds with the mercury electrode [7]. Cathodic stripping voltammetry of these compounds was utilised in determination of DNA and nucleic bases at nanomolar concentrations. In addition, adsorption/desorption processes of DNA at the mercury electrode provide distinct tensammetric peaks [8–12]. It has been shown that cathodic and tensammetric signals observed at mercury electrode respond sensitively to changes in the DNA structure [1,5,7,13].

* Corresponding author. Tel.: +420 5 41517142; fax: +420 5 41211293.
E-mail addresses: hasons@ibp.cz, voices@seznam.cz (S. Hasoň).

0039-9140/$ – see front matter © 2005 Elsevier B.V. All rights reserved.
doi:10.1016/j.talanta.2005.10.029

In DNA biosensors solid electrodes such as gold, carbon and indium–tin oxide have been used both for the DNA hybridisation and detection of the hybridisation event [14–19]. The mercury electrodes are not very popular among DNA biosensor developers due to drawback of classical hanging mercury drop electrode (HMDE) arising partly from problematic incorporation of these devices in miniaturised system and partly from poisonous liquid mercury. To overcome difficulties with DNA hybridisation at the hydrophobic mercury surface the double-surface technique has been proposed, in which DNA hybridisation is performed on one surface (magnetic beads) and electrochemical detection on another surface, the detection electrode (amalgam-alloy or graphite electrode) [12,20,21]. It means that still exist an emergency for development of the electrodes combining favourable features of the mercury and solid ones for their application in various fields of electroanalysis, including DNA sensor development. It seems that an appropriate alternative to the mercury electrode are either mercury film (MFE) or amalgam-alloy (MeAE) electrodes. Recently the MFEs and/or MeAEs have been introduced in two-dimensional condensation of the nucleic acid components [22–24] and also in DNA electroanalysis [25–29].

It has been shown that picomolar quantities of unlabeled DNA containing the purine units can be detected using the HMDE in the presence of copper [12,30]. Such a large increase in the sensitivity results from the acid hydrolysis of the DNA releasing purine bases from the DNA-chain. After acid hydrolysis of the DNA sample a better electrochemical accumulation of the complex of Cu(I) with a purine base residues (purine–Cu(I) complex) released from the DNA-chain on the electrode surface can take place. Nanomolar concentrations of the purine–Cu(I) complexes have been determined also at a silver or copper amalgam electrode modified by a liquid mercury meniscus [31]. In our previous paper, we adapted the above-mentioned electrochemical method based on the accumulation of the complex of Cu(I) with a purine base residues of acid hydrolysed oligodeoxynucleotide samples (ahODN–Cu(I) complex) at the mercury modified graphite/carbon electrode surfaces to the detection of different homopurine oligodeoxynucleotide lengths at a picomolar level (the detection of acid hydrolysed 80-mer (A_{80}) was possible down to 250 pM) [32].

In this paper, the electrochemically generated complex of Cu(I) with a purine base residues of acid hydrolysed oligodeoxynucleotide samples (ahODN–Cu(I) complex) we use to the: (a) detection of different oligodeoxynucleotide (ODN) lengths containing only purine (in our case the adenine) units, and (b) determination of the number of purine units within the 30-mer ODN samples containing a random sequence segments involving both the purine and pyrimidine units in connection with different solid amalgam-alloy electrodes. We show that an intensity of the cathodic stripping current density peak (j_{CSP}) of the electrochemically accumulated ahODN–Cu(I) complex increased linearly with increasing number of purine units in the ODN-chains used (the number of purine (adenine) units within the ODN-chains was changed from 10 to 80). A good correlation between the percentage content of purine units to the whole length of different 30-mer ODNs and the percentage content of the intensity of the j_{CSP} of the electrochemically accumulated 30-mer ahODN–Cu(I) complexes was observed as well. This method in combination with solid amalgam-alloy (MeAE) electrodes, similarly to the HMDE and/or MFE, is appropriate to detection of a picomolar concentration of unlabeled oligodeoxynucleotide samples containing purine units. This result confirms that the MeAEs provide at least one order of magnitude higher sensitivity in comparison with the carbon/graphite ones [33]. We also show that a sensitive analysis of acid-treated ODN in the presence of copper can be performed under a three-electrode electric circuit in 20-μl volumes of ODN at the MeAEs.

The above propose method of ODN determination at the MeAEs in the presence of copper can be used in current topic of DNA biosensors that are increasingly used for sequencing DNA by hybridisation. For instance, a detection of the number of repeat purine triplets in polynucleotides is important for confirming clinical diagnosis and for early recognition of heterozygous carriers because the genomic expansion of trinucleotide repetitive sequences is connected with inherited neurodegenerative diseases such as Friedreich ataxia [21,34].

2. Experimental

2.1. Instrumentation

The electrochemical measurements were performed with the AUTOLAB electrochemical system (Ecochemie, Utrecht, Netherlands) equipped with a potentiostat/galvanostat PGStat12. The working electrodes were different amalgam-alloy electrodes. A platinum wire and platinum plate (1 cm^2) served as the counter electrode during the measurement in the bulk solution and 20-μl droplet, respectively. The reference electrode was Ag|AgCl|3 M KCl.

An atomic force microscope (AFM) Nanoscope III (Veeco, Santa Barbara, California, USA) was used for the visualisation of the morphology and characterisation of the surface roughness of the mechanically polished and amalgamated gold polycrystalline electrode.

2.2. Chemicals

The electrochemical measurements were performed in 0.05 M sodium borate (pH 9.3). The solution was deaerated using 99.5% argon saturated with triply distilled water.

Oligodeoxynucleotides (ODNs), 10-mers (A_{10}), 25-mers (A_{25}), 50-mers (A_{50}), 80-mers (A_{80}), 5′TTCAAATCCTTCTCTAAATTTCTCTCAAAA3′ (P_{A10}), 5′TTTTTACTGGCCGTCGTTTTACTCTTTTCA3′ (P_{AG7}), 5′ATAACAATCAATAATACAATATCAAAAAAA3′ (P_{A20}), 5′GCGAGGTAAAACGACGGCCAGTCCTCGCTC3′ (P_{AG16}), and AAAAAAAAAAAAAAAAAAAAAAAAAAAAAA (P_{A30}) were purchased from Thermo Electron (Ulm, Germany). The ODNs concentrations related to the monomer were determined spectrophotometrically using a Libra S22 spectrophotometer. Hydrolysis of ODNs was performed by adding 60 μl of 0.5 M $HClO_4$ to samples of the same volume of ODNs at concentration of 5 μM and heating

for 30 min at 75 °C. After heating, the sample was cooled down, and neutralized with NaOH. Under these conditions only the purine bases are released from ODN-chain.

2.3. Electrode preparation and electrochemical modification

Gold, platinum, copper, and silver polycrystalline wires (diameter 1 mm) were obtained from Advent Research Materials Ltd (purity 99.999%). The metal wires were sealed into a glass tube with epoxy resin Torr-seal (Varian). The exposed ends of thus prepared electrodes were mechanically polished with 600-grit, 1200-grit, 2400-grit, 4000-grit silicon carbide papers (Struers) followed by polishing with 1-μm diamond paste (Leco) on Lecloth B polishing cloth (Leco). After polishing, the electrode was sonicated in triply distilled water (30 s).

The electrochemical modification of the metal electrodes was performed by the following procedure: (i) the first step includes the mercury plating on the mechanically polished and ultrasonically cleaned polycrystalline metal substrate from a 10 mM $Hg(NO_3)_2$ solution. The thicknesses of the mercury layers deposited on the metal substrates were controlled by a change deposition time t and current value I with respect to the Faraday law; (ii) the second step represents the cathodisation of the plated electrodes in the 0.2 M KCl solution bath at a constant potential of −2.20 V for 60 s. The application of a high negative potential results in hydrogen evolution and a decrease in the surface tension of mercury. It can be assumed, that after application of a high negative potential on the Hg-modified metal substrate, the liquid mercury has disappeared, and the Hg layer has been transformed into a solid amalgam-alloy [35,36]. The geometrical areas (A) of the amalgam-alloy electrodes were: $A = 0.008\ cm^2$.

3. Results and discussion

3.1. Optimisation of the measurement at the gold amalgam-alloy electrode (AuAE)

The propose electrochemical method of the voltammetric detection of different acid-treated oligodeoxynucleotides (ahODNs) containing the purine units within the ODN-chains in the presence of copper ions is based on the electrochemical accumulation of the complex of the purine base residues released from ODN-chains with copper ions Cu(I) (ahODN–Cu(I) complex) at the potential of reduction of copper ions Cu(II) followed the cathodic stripping of this complex from the MeAE surfaces. Therefore, we have studied how the change of some parameters can affect the measurement. The optimisation of the ahODN measurements at the AuAE includes the determination of the effects of: thickness of the amalgam-alloy layer (h), accumulation time (t_{AC}), stirring of the analysed solution (the number of revolutions of stirring rod, ω/min^{-1}), and amount of Cu(II) ions in the analysed solution ($c_{Cu(II)}$) on the cathodic stripping current density peak (j_{CSP}) of the electrochemically accumulated ahODN–Cu(I) complex. The influence of the above-mentioned parameters on the j_{CSP} of the ahODN–Cu(I) complex was tested

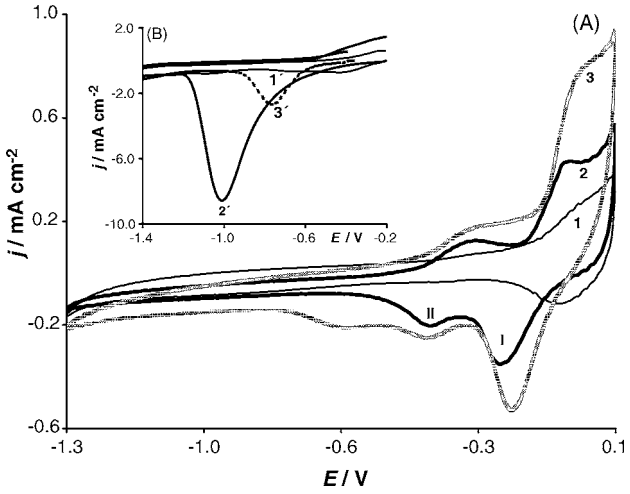

Fig. 1. (A) The steady state cyclic voltammograms (CVs) of: (1) 0.05 M sodium borate (pH 9.3); (2) 0.05 M sodium borate in the presence of 50 μM Cu(II); and (3) 0.05 M sodium borate in the presence of 25 nM acid hydrolysed 50-mer (A_{50}) + 50 μM Cu(II) on the 30 nm thick gold amalgam-alloy layer (30 nm AuAE). (B) The first CVs of 0.05 M sodium borate in the presence of: (1′) 50 μM Cu(II); and (2′ and 3′) 25 nM acid hydrolysed 50-mer (A_{50}) + 50 μM Cu(II) on the 30 nm AuAE. Before the potential scan the accumulation of the 25 nM (A_{50})–Cu(I) complex on the 30 nm AuAE was performed. The accumulation conditions were: potential of accumulation $E_{AC(I)} = -0.176$ V (1′ and 2′) and $E_{AC(II)} = -0.380$ V (3′); accumulation time of $t_{AC} = 10$ min; rate of stirring of the analysed solution $\omega = 3000\ min^{-1}$; scan rate of the measured CVs was $v_{scan} = 10\ V\ s^{-1}$. The measurement was performed at room temperature.

with 25 nM 50-mer (A_{50}) (the (A_{50}) contains the 50 adenine units).

The steady state cyclic voltammogram (CV) of 0.05 M sodium borate in the presence of 50 μM Cu(II) displays a two-electron reduction voltammetric signal of the copper ions on the 30 nm thick gold amalgam-alloy layer (30 nm AuAE) (Fig. 1(A), curve(2)). The first reduction peak (I) corresponding to the reduction of Cu(II) to Cu(I) is located at −0.20 V. The second peak (II) of the reduction reaction of Cu(I) to Cu(0) takes place at −0.38 V (Fig. 1(A), curve (2)). The steady state CV of 0.05 M sodium borate does not contain any voltammetric signals (Fig. 1(A), curve (1)). A broader part of CV of 0.05 M sodium borate at more positive potentials corresponds to the oxidation/reduction of the bulk (liquid) mercury at the gold amalgam-alloy surface (for details see Fig. 2). When ODN sample was added, the position of the reduction current peak (I) of Cu(II) is shifted to a more positive potential of −0.176 V (Fig. 1(A), curve (3)). We tested the possibility to use the potentials of reduction peaks I and II for electrochemical accumulation of the purine base residue–Cu(I) complex (ahODN–Cu(I) complex) at the 30 nm AuAE. From Fig. 1(B) it can be seen that after application of the accumulation potential of $E_{AC(I)} = -0.176$ V (peak I) a first CV scan of 25 nM 50-mer (A_{50}) in the presence of 50 μM Cu(II) on the 30 nm AuAE is characterised by a new, well-developed voltammetric peak at a potential of $E_{CSP} = -1.02$ V (Fig. 1(B), curve (2′)). This voltammetric signal is attributed to the stripping of the electrochemically accumulated ahODN–Cu(I) complex from the 30 nm AuAE. Similar results have been published previously for stripping of the purine base residue–Cu(I) complex accumulated at the HMDE [12,30],

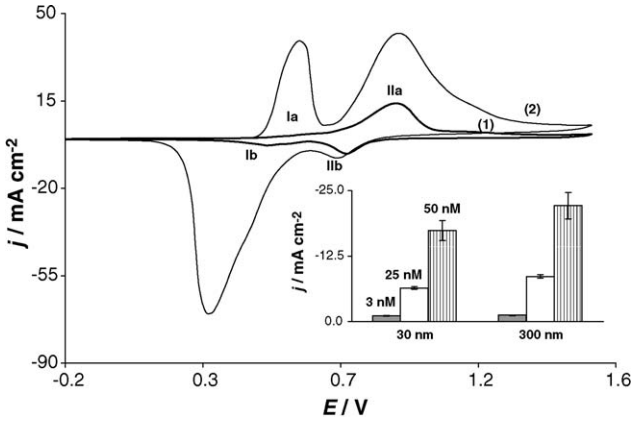

Fig. 2. The CVs of 0.05 M H_2SO_4 on the: (1) solid gold amalgam-alloy (30 nm AuAE) and (2) mercury film-modified gold amalgam-alloy (300 nm AuAE). The scan rate $v_{scan} = 0.1\ V\ s^{-1}$. The inset of Fig. 2 shows the current densities of the cathodic stripping peak (j_{CSP}) for three different concentration of (A_{50})–Cu(I) complex on both the solid (30 nm AuAE) and mercury film-modified (300 nm AuAE) gold amalgam-alloy electrode (the values of 50-mer (A_{50}) concentration are indicated in the figure). The values are mean ± standard deviations of five experiments. The accumulation conditions were: potential of accumulation $E_{AC(I)} = -0.176$ V; accumulation time of $t_{AC} = 10$ min; rate of stirring of the analysed solution $\omega = 3000\ min^{-1}$; scan rate of the measured CVs was $v_{scan} = 10\ V\ s^{-1}$.

and Hg-modified graphite electrodes [32]. A first CV scan of 0.05 M sodium borate in the presence of 50 μM Cu(II) does not contain any voltammetric signal under the same accumulation conditions (Fig. 1(B), curve (1′)). When the potential of second reduction peak II served as a accumulation potential ($E_{AC(II)} = -0.38$ V) the cathodic stripping current density peak (j_{CSP}) of the electrochemically accumulated 25 nM (A_{50})–Cu(I) complex was about 4.3-times lower and about of 260 mV positively shifted in comparison with the j_{CSP} for accumulation potential of $E_{AC(I)} = -0.176$ V (Fig. 1(B), curve (3′)). In the following experiments the potential of reduction peak I served as the accumulation potential ($E_{AC(I)}$) for the electrochemical generation of the ahODN–Cu(I) complex on the AuAE.

The nature of the gold amalgam-alloy was examined by anodic voltammetric stripping of the amalgam-alloy. The essentially solid gold amalgam-alloy (30 nm layer) produces a broad oxidation peak at +0.88 V (Fig. 2, peak(IIa), curve(1)), which arises due to the oxidation of an intermetallic compound of Au_2Hg and/or $AuHg_2$ [37,38]. On the other hand, the thick gold amalgam-alloy (300 nm layer) produced a new oxidation peak at about +0.57 V (Fig. 2, peak(Ia), curve(2)). This peak was attributed to the oxidation of bulk (liquid) mercury at the amalgam-alloy surface [37,39]. It was also observed that, with appearance of a new oxidation peak at +0.57, new reduction process emerged at +0.26 V (Fig. 2, peak(Ib), curve(2)). This peak can be attributed to the subsequent reduction of the formed Hg(II) species back to Hg(0) species. To the characterisation of the surface morphology of the thin and thick gold amalgam-alloy an atomic force microscope was used. To describe the electrode surface roughness we employed the root-mean-square function (RMS), defined as a standard deviation of the height and calculated from all points obtained during a given scan. Fig. 3(A) shows an AFM image of the polycrystalline gold mechanically polished with 1 μm abrasion particles with typical polishing lines (scratches) running all over the electrode surface. The mechanically polished polycrystalline gold has the RMS = 34.0 ± 0.5 nm. Fig. 3(B) shows that the surface of thin solid gold amalgam-alloy is characterised by inhomogeneously scattered mercury-amalgam nuclei of different diameter, which is distributed round about the polishing scratches. This surface becomes rougher and the RMS is 43 ± 3 nm. The density of the mercury-amalgam nuclei increases with increasing amalgamation time (Fig. 3(C)). It seems that for longer deposition times the smaller mercury-amalgam nuclei coalesce in real amalgam-alloy layer, which roughness increases to the value of RMS = 65 ± 5 nm (Fig. 3(D)). The inset of Fig. 2 shows the cathodic stripping current density peaks (j_{CSP}) of three different concentrations of the (A_{50}–Cu(I) complex) accumulated on the solid (30 nm AuAE) and mercury film-modified gold amalgam-alloy (300 nm AuAE), respectively. The heights of the j_{CSP} for lower and higher concentrations of (A_{50}) were about 7.8% and 30% higher for thick amalgam-alloy layer (300 nm AuAE) in comparison with thin one (30 nm AuAE).

The dependence of the j_{CSP} of (A_{50})–Cu(I) complex on the amount of copper ions in background solution ($c_{Cu(II)}$) exhibits a peak-shaped profile with maximum of 50 μM Cu(II) (not shown). The height of the j_{CSP} of (A_{50})–Cu(I) complex accumulated at the AuAE increases linearly with increasing accumulation time (t_{AC}) up to a value of $t_{AC} = 10$ min. For longer accumulation times ($t_{AC} > 10$ min) a limiting value of j_{CSP} was reached (not shown). It was observed that the stirring of the analysed solution accelerated the transport of the electroactive species to the electrode surface and the large quantity of (A_{50})–Cu(I) complex is formed on the AuAE under controlled potential (not shown). The reproducibility of the maximum of j_{CSP} for 25 nM (A_{50}) on the 30 nm AuAE was tested. The average value was $j_{CSP} = -6.53 \pm 0.23\ mA\ cm^{-2}$ (relative standard deviation, RSD = 4.0%, number of measurements $n = 10$).

3.2. *Detection of oligodeoxynucleotides containing only purine units with different lengths in the bulk solution at the gold amalgam-alloy electrodes in the presence of Cu(II)*

Firstly, the influence of length of ahODN samples containing only a different number of adenine units (the number of adenine units was changed from 10 to 80) on the behaviour of the cathodic stripping current density peaks (j_{CSP}) of the electrochemically accumulated ahODN–Cu(I) complexes at the 30 nm (Fig. 4, full circle) and 300 nm AuAE (Fig. 4, full square) substrates was studied (the concentration of each ahODN used was kept at 50 nM). Fig. 4 shows that the j_{CSP} of ahODN–Cu(I) complexes increases linearly with the length of ahODNs used for both the 30 nm and 300 nm AuAE (the correlation coefficients were: $R^2 = 0.986$ (30 nm AuAE) and $R^2 = 0.989$ (300 nm AuAE). The thickness of the gold amalgam-alloy layer has a larger influence on the height of j_{CSP} for longer ahODN samples (Fig. 4). The values of the j_{CSP} of (A_{10})–Cu(I) and (A_{80})–Cu(I) complexes are about 1% and 30% higher for

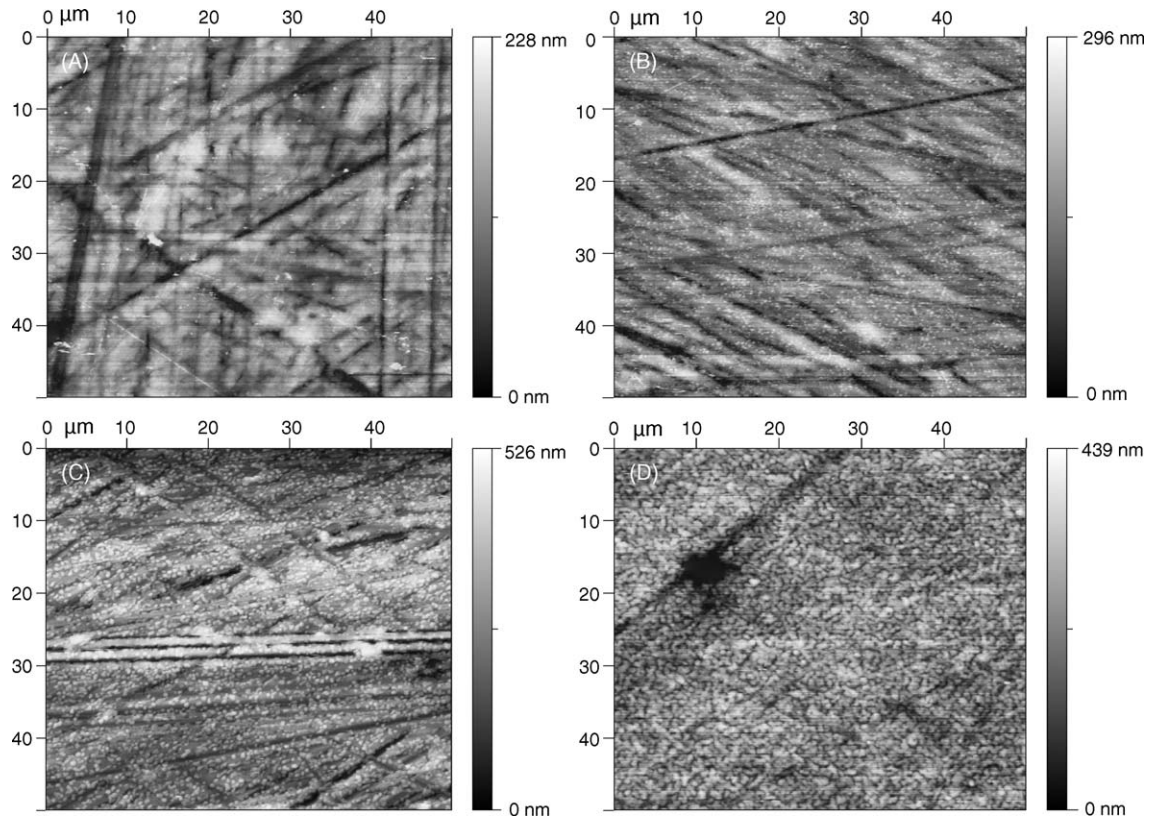

Fig. 3. AFM images of the: (A) polycrystalline gold mechanically polished with 1 μm abrasion particles; (B) solid gold amalgam-alloy (approximately 30 nm layer); (C) 100 nm gold amalgam-alloy; and (D) mercury film-modified gold amalgam-alloy (approximately 300 nm layer).

the 300 nm AuAE contrary to 30 nm AuAE, respectively. The linear dependence of the j_{CSP} on the ahODN length for lower concentrated ahODN samples ($c = 25$ nM) at the 30 nm AuAE was observed as well (Fig. 4 (full triangle); $R^2 = 0.997$). If the voltammetric analysis of the acid-treated ODNs is carried out in the bulk solution then the position of the j_{CSP} of ahODN–Cu(I) complexes is clearly shifted to more negative potential with the increasing length of ahODNs used (the inset of Fig. 4).

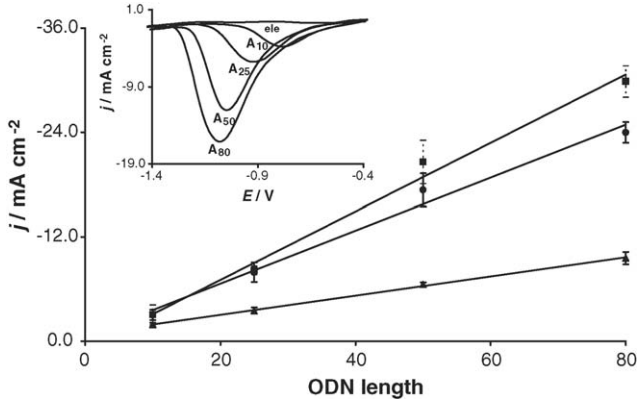

Fig. 4. The dependence of the current density of the cathodic stripping peak (j_{CSP}) of: (●), 50 nM; (▲), 25 nM ahODN–Cu(I) complexes accumulated at the 30 nm AuAE; and (■) 50 nM ahODN–Cu(I) complexes accumulated at the 300 nm AuAE on the lengths of acid hydrolysed ODN (ahODN) samples containing only adenine units. The values are mean ± standard deviations of five experiments. The inset shows the parts of cyclic voltammograms of 50 nM ahODN samples of different lengths in 0.05 M sodium borate in the presence of 50 μM Cu(II) on the 30 nm AuAE. (ele) Represents the response of 0.05 M sodium borate in the presence of 50 μM Cu(II) recorded under the same conditions. The length of ahODNs expressed as the number of adenine bases is indicated in the figure. The accumulation conditions were the same as in Fig. 2.

For the 10-mer (A_{10}) and 80-mer (A_{80}) the concentration dependences were measured. From Fig. 5(A) it can be seen that acid hydrolysed 80-mer (A_{80}) is still detectable down to 200 pM. It means that the sensitivity of the voltammetric detection of ahODNs at the solid amalgam-alloy is similar to the Hg-modified graphite electrode [32] and at least one order of magnitude higher in comparison with the carbon/graphite electrodes. Fig. 5(B) shows that the linear dependence of the j_{CSP} on the (A_{80}) concentration in the range from 0.2 nM to 50 nM is observed (the correlation coefficient was $R^2 = 0.994$, full triangle). On the other hand, at higher concentrations ($c > 60$ nM) the height of the j_{CSP} of (A_{80})–Cu(I) complex reaches a limiting value of $j_{CSP} = -16.3$ mA cm^{-2}. In the case of 10-mer (A_{10}) the linear concentration dependence of the j_{CSP} in the range from 5 nM to 100 nM with the detection limit of 5 nM was observed (Fig. 5(B), full circle).

3.3. Determination of the number of purine units within the 30-mer ODNs in the bulk solution at the gold amalgam-alloy electrodes in the presence of Cu(II)

We also applied the proposed electrochemical method for determination of the number of purine (adenine and/or

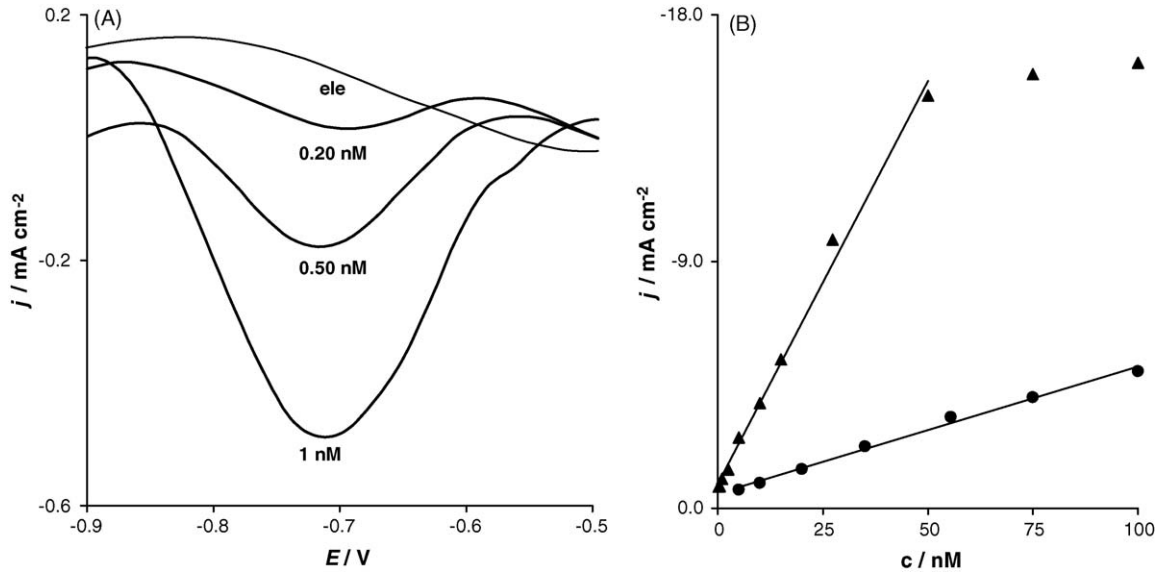

Fig. 5. (A) The parts of baseline corrected cyclic voltammograms of acid hydrolysed 80-mer (A_{80}) at lower concentrations (the values of 80-mer (A_{80}) concentration are indicated in the figure) in 0.05 M sodium borate in the presence of 50 μM Cu(II) on the 30 nm AuAE. (ele) Represents the response of 0.05 M sodium borate in the presence of 50 μM Cu(II) recorded under the same conditions. (B) The dependences of the j_{CSP} of: (●) (A_{10})–Cu(I) and (▲) (A_{80})–Cu(I) complexes accumulated at the 30 nm AuAE on the concentration of acid hydrolysed 10-mer (A_{10}) and 80-mer (A_{80}), respectively. The accumulation conditions were the same as in Fig. 2.

adenine + guanine) units within the 30-mer ODNs containing both the purine and pyrimidine units. We used 50 nM of five different 30-mer ODNs. The samples P_{A10} and P_{A20} contain a random sequence segments involving 10 and 20 adenine units (the ODNs not contain the guanine segments), respectively. The P_{AG7} and P_{AG16} contain also random segments involving 3 adenine + 4 guanine and 7 adenine + 9 guanine, respectively. P_{A30} contains only 30 adenine units. It can be seen from Fig. 6(A) that the position of the j_{CSP} is shifted to more negative potential with the increasing number of purine units within the 30-mer ODNs as well. Fig. 6(B) shows a correlation between the percentage content of purine (adenine and/or adenine + guanine) units within the different 30-mer ODNs (white columns) and the percentage content of the intensity of the j_{CSP} of the electrochemically accumulated ahODN–Cu(I) complexes (grey columns). If the signal obtained with P_{A30} (30-mer involving only purine (adenine) units) was taken as 100% then the height of the j_{CSP} exhibiting 62.5%, 49.7%, 37.5%, and 27.4% for 30-mer ODNs P_{A20} (30-mer involving 20 adenine units), P_{AG16} (30-mer involving 7 adenine and 9 guanine units), P_{A10} (30-mer involving 10 adenine units), and P_{AG7} (30-mer involving 3 adenine and 4 guanine units), respectively. These values were in agreement with the ratio of number of the purine units to the whole length of ODN samples (Fig. 6(B), white columns). It can be concluded that only the purine units are participate in a reaction with copper ions and pyrimidine ones are inactive with respect to the procedure used. To the differentiation of adenine and guanine units within the acid-treated ODN it will be necessary to apply the carbon/graphite electrodes because, as it was shown previously [33], the height of oxidation signal of adenine and/or guanine residues of acid-treated ODN sensitively increases after accumulation of the ahODN–Cu(I) complex.

3.4. Detection of different oligodeoxynucleotides in the 20-μl solution droplet at the gold amalgam-alloy electrodes in the presence of Cu(II)

In this section the voltammetric analysis of different ahODNs is carried out in 20-μl droplet of the analysed solution. For

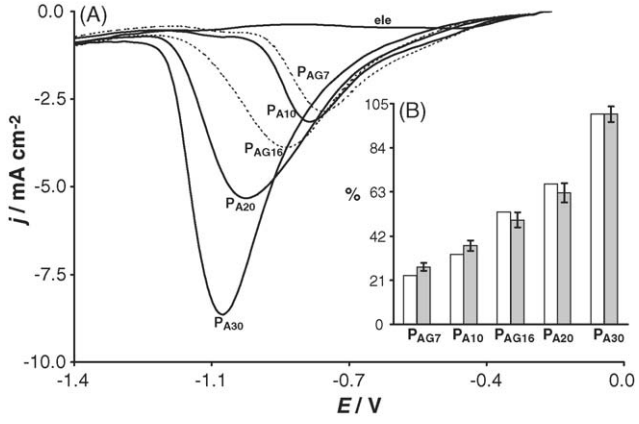

Fig. 6. (A) The parts of first CVs of 50 nM acid hydrolysed 30-mer ODNs in 0.05 M sodium borate in the presence of 50 μM Cu(II) at the 30 nm AuAE. The samples P_{A10} and P_{A20} contain a random sequence segments involving 10 and 20 adenine units (the ODNs not contain the guanine segments), respectively. The P_{AG7} and P_{AG16} contain also random segments involving 3 adenine + 4 guanine and 7 adenine + 9 guanine, respectively. P_{A30} contains only 30 adenine units. (B) The white columns represent the percentage content of purine (adenine and/or adenine + guanine) units within five different 30-mer ODNs. The P_{A30} ODN containing only purine (adenine) units served as 100%. The grey columns represent the percentage content of the intensity of the j_{CSP} of five 30-mer ODNs used. The height of the j_{CSP} of P_{A30} ODN was taken as 100% as well. The values are mean ± standard deviations of five experiments. (ele) Represents the response of 0.05 M sodium borate in the presence of 50 μM Cu(II) recorded under the same conditions. The accumulation conditions were the same as in Fig. 2.

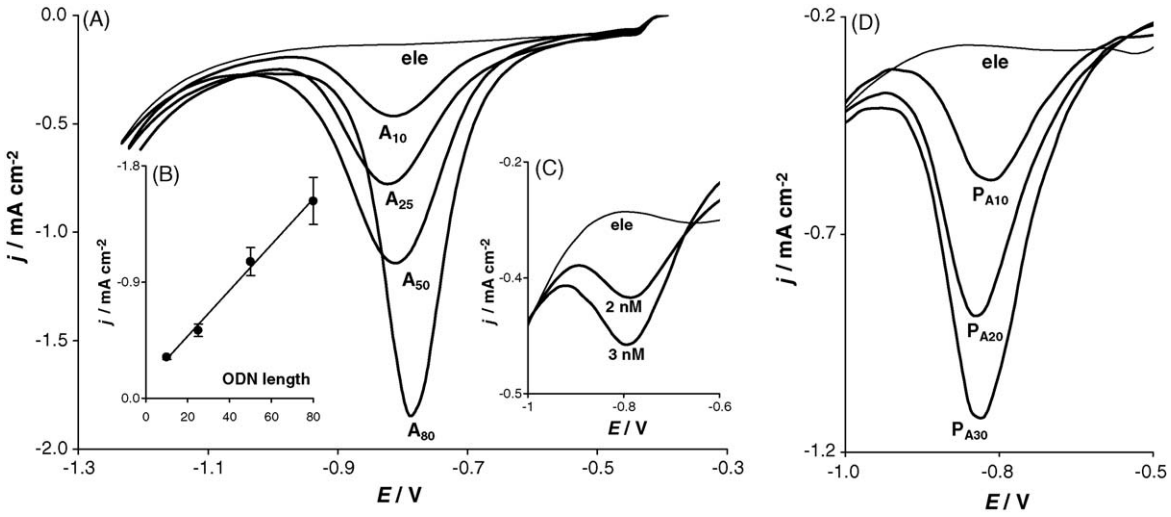

Fig. 7. (A) The parts of first CVs of 50 nM ahODNs of different lengths containing only adenine units in a 20-μl droplet of 0.05 M sodium borate in the presence of 50 μM Cu(II) on the 30 nm AuAE. The lengths of ahODNs expressed as the number of adenine bases are indicated in the figure. (B) The dependence of the j_{CSP} of ahODN–Cu(I) complexes accumulated at the 30 nm AuAE from a 20-μl droplet on the lengths of ahODNs. (C) The parts of baseline corrected first CVs of acid hydrolysed 80-mer (A_{80}) at lower concentrations (the concentrations are indicated in the figure) in a 20-μl droplet of 0.05 M sodium borate in the presence of 50 μM Cu(II) on the 30 nm AuAE. (D) The parts of first CVs of 50 nM acid hydrolysed 30-mer ODNs in 20-μl droplet of 0.05 M sodium borate in the presence of 50 μM Cu(II) on the 30 nm AuAE. The samples P_{A10} and P_{A20} contain a random sequence segments involving 10 and 20 adenine units, respectively. P_{A30} contains only 30 adenine units. (ele) Represents the response of 0.05 M sodium borate in the presence of 50 μM Cu(II) recorded under the same conditions. The accumulation conditions were: potential of accumulation $E_{AC(I')} = -0.38$ V; accumulation time of $t_{AC} = 10$ min; scan rate $v_{scan} = 10$ V s^{-1}.

a microanalysis a three-electrode connection was applied as well. The analysed 20 μl-droplet of the ahODN was placed on the platinum plate (1 cm^2), which served as the counter electrode. The exposed ends of the working and reference electrodes were immersed into the analysed ahODN droplet. During the potential-controlled accumulation of the ahODN–Cu(I) complexes on the AuAE substrate from a 20-μl droplet we applied a fast-scan voltammetry as a strategy to avoid the oxygen interference in the un-deaerated and/or un-stirred solution [40,41].

Fig. 7(A) shows that the potential of the j_{CSP} of the electrochemically accumulated ahODN–Cu(I) complexes from a 20-μl droplet is almost independent on the increasing length of ahODN used. Note, that the accumulation potential ($E_{AC(I')}$) for the electrochemical generation of the ahODN–Cu(I) complex at the AuAE from 20-μl volume was about 200 mV negatively shifted in comparison with the bulk solution. The heights of the j_{CSP} of the electrochemically accumulated ahODN–Cu(I) complexes from a 20-μl ahODN droplet increased also linearly with the length of ahODNs containing only different number of adenine units (Fig. 7(B); the concentration of each ahODN used was kept at 50 nM; correlation coefficient $R^2 = 0.993$). When the analysis is carried out in the 20-μl droplets then the detection of acid hydrolysed 80-mer (A_{80}) is possible down to 2 nM (Fig. 7(C)). The determination of the number of purine units within the 30-mer ODNs containing both the purine and pyrimidine units in the 20-μl ODN droplets was utilised as well. Fig. 7(D) shows a good correlation between the number of adenine units within the 30-mer ODNs and the heights of the j_{CSP} of the electrochemically accumulated ahODN–Cu(I) complexes.

3.5. Detection of oligodeoxynucleotides on the different amalgam-alloy electrodes in the presence of Cu(II)

In this paragraph a behaviour of the j_{CSP} of the 5 nM (A_{80})–Cu(I) complex on four different amalgam-alloy surfaces was studied. In the case of the gold (AuAE), platinum (PtAE), and copper amalgam-alloy (CuAE) electrode a well-developed j_{CSP} of 5 nM (A_{80})–Cu(I) complex at a potential of $E_{CSP(AuAE)} = -0.78$ V (Fig. 8(A)), $E_{CSP(PtAE)} = -0.87$ V (Fig. 8(B)), $E_{CSP(CuAE)} = -0.89$ V (Fig. 8(C)) has appeared, respectively. The corresponding accumulation potentials were $E_{AC(AuAE)} = -0.176$ V, $E_{AC(PtAE)} = -0.321$ V, and $E_{AC(CuAE)} = -0.358$ V. The first CVs of 0.05 M sodium borate in the presence of 50 μM Cu(II) with and without addition of 5 nM 80-mer (A_{80}) at the silver amalgam-alloy electrode (AgAE) display similar voltammetric peaks at the potential of $E_{CSP(AgAE)} = -0.99$ V (Fig. 8(D)). The accumulation potential on the AgAE was $E_{CSP(AgAE)} = -0.375$ V. Because the 0.05 M sodium borate in the presence of 50 μM Cu(II) at the AgAE produces a voltammetric signal similar to the 5 nM (A_{80})–Cu(I) complex the AgAE cannot be used for the detection of the lower concentration of the ahODNs. This result differs from recently published data about cathodic stripping voltammetric determination of free purine bases in the presence of copper ions on the polished and mercury film-modified silver solid amalgam electrodes [29,42]. Explanation of this disproportion is not easy because our experimental conditions (procedure of preparation of an amalgam-alloy electrode, background electrolyte, quantity of copper ions) are different from that published in Ref [29,31,42]. In addition, we refer about AgAE only with respect to use of different amalgam-alloy electrodes.

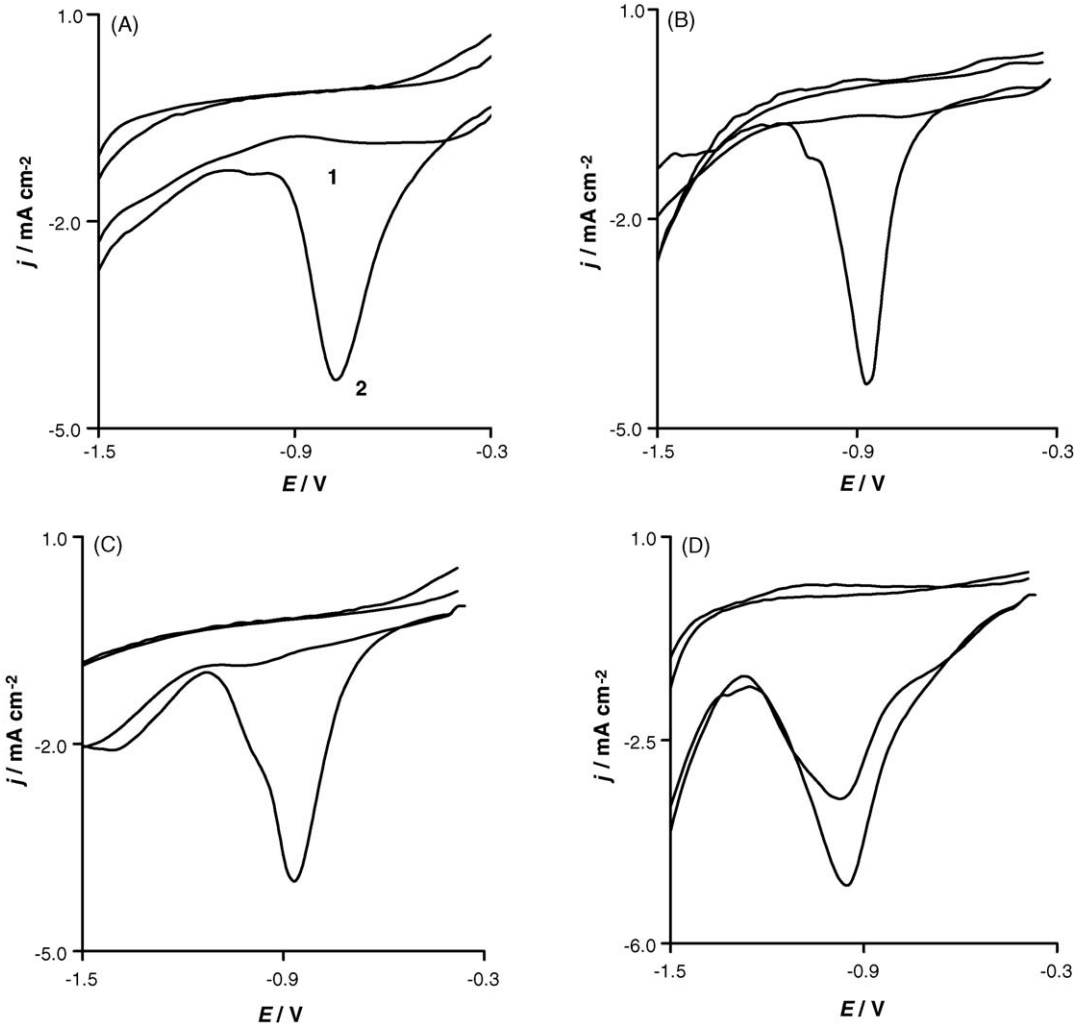

Fig. 8. The first CVs of: (1) 0.05 M sodium borate in the presence of 50 μM Cu(II); and (2) 5 nM 80-mer (A_{80}) in 0.05 M sodium borate in the presence of 50 μM Cu(II) on the: (A) 100 nm gold (AuAE); (B) 100 nm platinum (PtAE); (C) 100 nm copper (CuAE); and (D) 100 nm silver amalgam-alloy electrode (AgAE). The accumulation conditions were: potential of accumulation $E_{AC(AuAE)} = -0.176$ V (A); $E_{AC(PtAE)} = -0.321$ V (B); $E_{AC(CuAE)} = -0.358$ V (C); and $E_{AC(AgAE)} = -0.375$ V (D); accumulation time of $t_{AC} = 10$ min; rate of stirring of the analysed solution $\omega = 3000\ \text{min}^{-1}$; scan rate $\upsilon_{scan} = 10\ \text{V s}^{-1}$.

4. Conclusion

It was shown that the gold, platinum, and copper amalgam-alloy electrodes are a good alternative to a hanging mercury drop electrode and/or mercury film-modified graphite electrodes for a sensitive voltammetric detection of the acid hydrolysed oligodeoxynucleotides containing the purine units in the presence of copper ions. The analysis of the ahODNs was based on the cathodic stripping of the electrochemically accumulated complex of Cu(I) with a purine base residues released from ODN-chain during acid hydrolysis of the ODNs (ahODN–Cu(I) complex) from the amalgam-alloy surface. We were able to detect the 200 pM and 2 nM of acid hydrolysed 80-mer (A_{80}) in the bulk solution and in 20-μl droplet of the (A_{80}) sample at the gold amalgam-alloy (AuAE) electrode, respectively. We showed that the intensity of the cathodic stripping current peak (j_{CSP}) of the electrochemically accumulated ahODN–Cu(I) complexes increased linearly with increasing number of purine units in the ODN-chains used (the number of purine (adenine) units within the ODN-chains was changed from 10 to 80) not only in the bulk solution, but also in 20-μl volume of analysed sample. A good correlation between the percentage content of purine units to the whole length of different 30-mer ODNs and the percentage content of the intensity of the j_{CSP} of the electrochemically accumulated 30-mer ahODN–Cu(I) complexes was observed as well. We provide at least one order of magnitude higher sensitivity of unmodified ahODN detection at the solid amalgam-alloy electrodes in comparison with the carbon/graphite ones.

Acknowledgements

This work was supported by the Grant Agency of the Academy of Sciences of the Czech Republic KJB 4004305 (S.H.), A4004404 (V.V.), S5004107 (V.V.), and institutional grant Z 5004920. The authors wish to thank Dr. Petr Klapetek (Czech Metrology Institute, Brno, Czech Republic) for his help in obtaining the AFM data and Mr. M. Hasoň for his technical assistance.

References

[1] E. Paleček, M. Fojta, Anal. Chem. 73 (2001) 74A.
[2] J. Wang, Anal. Chim. Acta 500 (2003) 247.
[3] T.G. Drummond, M.G. Hill, J.K. Barton, Nat. Biotechnol. 21 (2003) 1192.
[4] J. Wang, Anal. Chim. Acta 469 (2002) 63.
[5] M. Fojta, Electroanalysis 14 (2002) 1449.
[6] P. de-los-Santos-Alvarez, M.J. Lobo-Castanon, A.J. Miranda-Ordieres, P. Tunon-Blanco, Anal. Bioanal. Chem. 378 (2004) 104.
[7] E. Paleček, M. Fojta, F. Jelen, V. Vetterl, in: A.J. Bard, M. Stratsmann (Eds.), G.S. Wilson (Series Ed.), The Encyclopedia of Electrochemistry, vol. 9, Wiley-VCH, Weinheim, 2002, pp. 365–429.
[8] E. Paleček, Anal. Biochem. 108 (1980) 129.
[9] E. Paleček, F. Jelen, M.A. Hung, J. Lasovsky, Bioelectrochem. Bioenerg. 8 (1981) 621.
[10] E. Paleček, J. Osteryoung, R.A. Osteryoung, Anal. Chem. 54 (1982) 1389.
[11] E. Paleček, S. Billová, L. Havran, R. Kizek, A. Mičulková, F. Jelen, Talanta 56 (2002) 919.
[12] F. Jelen, B. Yosypchuk, A. Kouřilová, L. Novotný, E. Paleček, Anal. Chem. 74 (2002) 4788.
[13] M. Fojta, Collect. Czech. Chem. Commun. 69 (2004) 715.
[14] M.J. Tarlov, A.B. Steel, in: J.F. Rusling (Ed.), Biomolecular Films. Design, Function, and Applications, Marcel Dekker, New York, 2003, pp. 545–608.
[15] N. Popovich, H.H. Thorp, Interface 11 (2002) 30.
[16] H. Wackerbarth, M. Grubb, J. Zhang, A.G. Hansen, J. Ulstrup, Langmuir 20 (2004) 1647.
[17] D.Y. Petrovykh, H. Kimura-Suda, L.J. Whitman, M.J. Tarlov, J. Am. Chem. Soc. 125 (2005) 5219.
[18] H.H. Thorp, Long-Range Charge Transfer in DNA; Topics in Current Chemistry 237, Springer-Verlag, Heidelberg, 2004, pp. 159–181.
[19] E. Katz, I. Willner, Electroanalysis 15 (2003) 913.
[20] E. Paleček, M. Fojta, F. Jelen, Bioelectrochemistry 56 (2002) 85.
[21] M. Fojta, L. Havran, R. Kizek, S. Billová, E. Paleček, Biosens. Bioelectron. 20 (2004) 985.
[22] S. Hasoň, V. Vetterl, J. Electroanal. Chem. 536 (2002) 19.
[23] S. Hasoň, S.-P. Simonaho, R. Silvennoinen, V. Vetterl, Electrochim. Acta 48 (2003) 651.
[24] S. Hasoň, S.P. Simonaho, R. Silvennoinen, V. Vetterl, J. Electroanal. Chem. 568 (2004) 65.
[25] T. Kubicarova, M. Fojta, J. Vidic, M. Tomschik, D. Suznjevic, E. Palecek, Electroanalysis 12 (2000) 1390.
[26] T. Kubicarova, M. Fojta, J. Vidic, L. Havran, E. Palecek, Electroanalysis 12 (2000) 1422.
[27] S. Hasoň, J. Dvořák, F. Jelen, V. Vetterl, Crit. Rev. Anal. Chem. 32 (2002) 167.
[28] K. Kucharikova, L. Novotny, B. Yosypchuk, M. Fojta, Electroanalysis 16 (2004) 410.
[29] R. Fadrna, K. Cahova-Kucharikova, L. Havran, B. Yosypchuk, M. Fojta, Electroanalysis 17 (2005) 452.
[30] F. Jelen, A. Mičulková, P. Pečinka, E. Paleček, Bioelectrochemistry 63 (2004) 249.
[31] B. Yosypchuk, M. Heyrovský, E. Paleček, L. Novotný, Electroanalysis 14 (2002) 1488.
[32] S. Hasoň, F. Jelen, L. Fojt, V. Vetterl, J. Electroanal. Chem. 577 (2005) 263.
[33] L. Fojt, S. Hasoň, J. Electroanal. Chem., in press.
[34] M. Fojta, L. Havran, M. Vojtiskova, E. Palecek, J. Am. Chem. Soc. 126 (2004) 6532.
[35] A.M. Hartley, A.G. Hiebert, J.A. Cox, J. Electroanal. Chem. 17 (1968) 81.
[36] J.F. Goelz, W.R. Heineman, J. Electroanal. Chem. 103 (1979) 147.
[37] J.B. Brown, J. Chem. Educ. 37 (1960) 415.
[38] A. Beer, Y. Lereah, A. Frydman, H. Taitelbaum, Physica A 314 (2002) 325.
[39] C.M. Welch, O. Nekrassova, X. Dai, M.E. Hyde, R.G. Compton, Chem. Phys. Chem. 5 (2004) 1405.
[40] A.S. Baranski, Anal. Chem. 59 (1987) 662.
[41] J.O. Howell, R.M. Wightman, Anal. Chem. 56 (1984) 524.
[42] R. Fadrná, B. Yosypchuk, M. Fojta, T. Navrátil, L. Novotný, Anal. Lett. 37 (2004) 399.